

VEDIT: LATENT PREDICTION ARCHITECTURE FOR PROCEDURAL VIDEO REPRESENTATION LEARNING

Anonymous authors

Paper under double-blind review

ABSTRACT

Procedural video representation learning is an active research area where the objective is to learn an agent which can anticipate and forecast the future given the present video input, typically in conjunction with textual annotations. Prior works often rely on large-scale pretraining of visual encoders and prediction models with language supervision. However, the necessity and effectiveness of extending compute intensive pretraining to learn video clip sequences with noisy text supervision have not yet been fully validated by previous works. In this work, we show that a strong off-the-shelf frozen pretrained visual encoder, along with a well designed prediction model, can achieve state-of-the-art (SoTA) performance in forecasting and procedural planning without the need for pretraining the prediction model, nor requiring additional supervision from language or ASR. Instead of learning representations from pixel space, our method utilizes the latent embedding space of publicly available vision encoders. By conditioning on frozen clip-level embeddings from observed steps to predict the actions of unseen steps, our prediction model is able to learn robust representations for forecasting through iterative denoising —leveraging the recent advances in diffusion transformers (Peebles & Xie, 2023). Empirical studies over a total of five procedural learning tasks across four datasets (NIV, CrossTask, COIN and Ego4D-v2) show that our model advances the strong baselines in long-horizon action anticipation (+2.6% in Verb ED@20, +3.1% in Noun ED@20), and significantly improves the SoTA in step forecasting (+5.0%), task classification (+3.8%), and procedure planning tasks (up to +2.28% in success rate, +3.39% in mAcc, and +0.90% in mIoU).

1 INTRODUCTION

Humans regularly perform complex, multi-step *procedural* activities with ease (e.g., cooking a recipe, assembling a piece of furniture). This ability stems from our capacity to recognize, reason about and plan for these activities, which is crucial for developing effective embodied AI systems to perform similar tasks. Towards this, designing systems that can understand procedural activities and predict the next logical steps is an active research problem (Brohan et al., 2023; Chang et al., 2020; Tellex et al., 2011). On the one hand, a large body of prior work on visual representation learning demonstrates the importance of large-scale image or video pretraining for single-step activity understanding (Oquab et al., 2024; Bardes et al., 2024; Zhai et al., 2023; Wang et al., 2023c; Chen et al., 2021; Assran et al., 2023; Xu et al., 2024). On the other hand, encoding sequences of steps (*i.e.*, building a *prediction model*) for future step prediction in videos is a relatively new area of research. Existing procedural video representation learning approaches (Lin et al., 2022; Zhong et al., 2023) typically inherit the same methodology as traditional activity understanding from single short video clip — extending [single-clip pretraining](#) to large-scale [pretraining on video clip sequences](#) (e.g., in HowTo100M (Miech et al., 2019)) with generic objectives, such as masked step prediction supervised by noisy ASR annotations obtained from narrated videos (Shvetsova et al., 2024) or fixed text knowledge bases like wikiHow (Koupae & Wang, 2018).

However, the necessity and effectiveness of [pretraining the prediction model on video clip sequences](#) have not yet been fully validated in these works for two main reasons. First, the dominant [single-clip pretraining](#) objectives (e.g., masked token prediction) were designed for feature learning of a short single clip, and are not well aligned to the breadth of downstream procedural tasks (e.g., step forecasting, task classification, procedural planning). Second, [pretraining for sequences](#) rather

than single steps demands a scale of data beyond what is currently available. As a result, current approaches (Lin et al., 2022; Zhong et al., 2023) fall back on text annotations that are often noisy and poorly temporally aligned with the video content (e.g., ASR narrations). Therefore, in this work, we investigate how far an approach can go without requiring extensive [pretraining on video clip sequences](#). Our hypothesis is that learning an efficient prediction model (i.e., transition function) over strong abstract representations from frozen visual encoders offers a compelling alternative to extensive large-scale [video clip sequences pretraining](#) for procedural learning tasks.

To this end, we propose our framework **VEDiT - Video Embedding Diffusion Transformer** – a scalable diffusion transformer (DiT, Peebles & Xie (2023))-based prediction model to encode multi-step procedural videos. VEDiT inherits both the diffusion-style training objective and architecture. Specifically, during training, we utilize the latest Flow Matching technique (Esser et al., 2024; Lipman et al., 2023; Goodfellow et al., 2016) for iterative denoising from random Gaussian noise into video clip embeddings. Unlike DiT-based models designed for fine-grained image/video generation (Yang et al., 2024; Esser et al., 2024) which operate at the patch level, our prediction model works as the step/state transition function, utilizing the abstract frame-level representations from frozen visual encoders, operating in latent space (LeCun, 2022). This abstraction allows our model to capture the temporal aspects of the procedural learning task, resulting in the ability to learn an efficient transition function. Crucially, our method *does not require pre-training* as it utilizes existing pre-trained representations, nor does it rely on additional supervision (from text or ASR).

We evaluate our model on five diverse procedural learning tasks across four datasets. (1) On the COIN (Tang et al., 2019) dataset, our model outperforms previous SoTA by a large margin (+5.0% for step forecasting and +3.8% for task classification), and demonstrates scalable learning as we increase the model size. (2) Our newly proposed VEDiT significantly enhances the overall performance of previous SoTA (Niu et al., 2024) on procedure learning tasks on NIV (Alayrac et al., 2016), CrossTask (Zhukov et al., 2019), and COIN (up to +2.28% in success rate, +3.39% in mean accuracy, and +0.90% in mean IoU), as well as the strong baseline for the Ego4D-v2 (Grauman et al., 2022) long-horizon action anticipation task (+2.6% in Verb ED@20, +3.1% in Noun ED@20). (3) Finally, we conduct detailed ablation studies on the choice of visual encoders, architecture ablations and large-scale [pretraining on video clip sequences](#), and confirm the effectiveness of each component of our framework design.

In a nutshell, our main contributions can be summarized as follows:

- We propose a procedural video representation learning framework (VEDiT) which leverages diffusion transformers to predict visual representations entirely in the embedding space.
- By combining strong pretrained visual encoders [on single video clips](#) with a simple prediction model design, our framework is designed to be trained effectively on a single cross-entropy loss for downstream tasks, eliminating the need for large-scale [pretraining on video clip sequences](#) and additional supervision from actions labels or language for learning the prediction model.
- We evaluate VEDiT on five downstream tasks, including step classification, step forecasting, task classification, procedure planning, and long-term action anticipation across four widely-used benchmark datasets. Our framework outperforms previous SoTAs and baselines by a large margin.

2 RELATED WORKS

Procedural Video Understanding. Learning procedural knowledge from videos has become an active research area, driven by recent large-scale datasets (Miech et al., 2019; Sener et al., 2022; Afouras et al., 2024; Song et al., 2024) and models trained on them (Niu et al., 2024; Wang et al., 2023a;b; Zhao et al., 2022; Lin et al., 2022; Zhong et al., 2023). These models often rely heavily on large-scale text supervision. For example, DistantSup (Lin et al., 2022) creates text supervision by linking step descriptions from a textual knowledge base (wikiHow) (Koupae & Wang, 2018) to text narrations from ASR in videos. ProceduralVRL (Zhong et al., 2023) aligns ASR narration embeddings to video representations using strong pretrained image-language models (Radford et al., 2021). Moreover, prior work uses architectures that necessitate large-scale [pretraining on video clip sequences](#) (e.g., self-attention transformers in ProceduralVRL). In contrast, we propose an efficient architecture that learns directly from video, side-stepping the requirement for large-scale language annotations or [pretraining on video clip sequences](#).

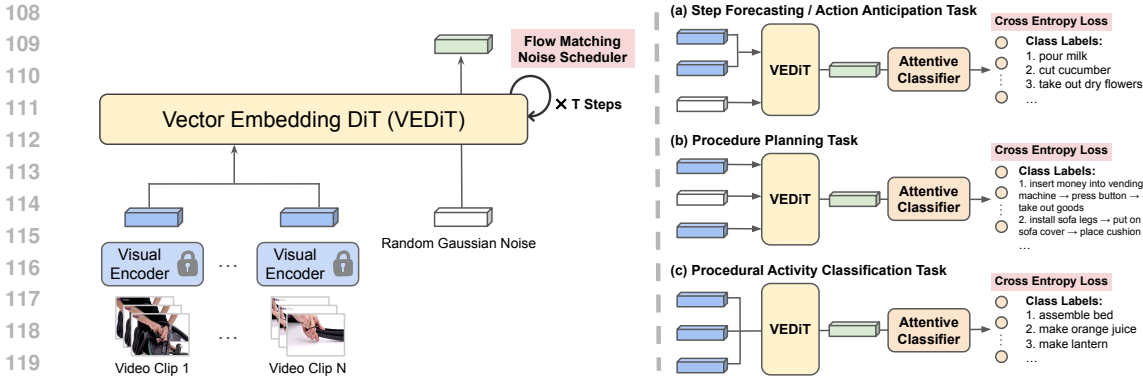


Figure 1: **Overview of our VEDiT training pipeline.** **Model architecture (left):** We introduce *masked clip-level latent prediction* as our training objective, where we train a Vector Embedding DiT (VEDiT) to iteratively denoise T steps from random gaussian noise with flow matching noise scheduler. **Downstream tasks (right):** We train VEDiT with a light-weight attentive classifier (Bardes et al., 2024) with cross-entropy loss for the following tasks. (a) *Step forecasting / action anticipation task*: predict the embeddings of next unseen clip from observed clips with VEDiT. (b) *Procedure planning task*: predict the embeddings of intermediate unseen clips from observed starting and goal clips with VEDiT. (c) *Procedural activity classification task*: given a sequence of observed video clips, predict the label of the procedural video.

Diffusion Transformers and Flow Matching. Diffusion models (Song et al., 2020a; Ho et al., 2020; Sohl-Dickstein et al., 2015; Song et al., 2020b) have emerged as a new state-of-the-art architecture for deep generative models. Compared with UNet-based diffusion models (Rombach et al., 2022; Blattmann et al., 2023), recent architectures (Ma et al., 2024c; Chen et al., 2024; Esser et al., 2024; Gao et al., 2024; Yang et al., 2024) designed based on diffusion transformers (Peebles & Xie, 2023) have achieved significant success and scalability in image and video generation. On the other hand, flow matching (Lipman et al., 2023; Ma et al., 2024b; Karras et al., 2022; Nichol & Dhariwal, 2021) has shown great potential as an alternative to DDPM (Nichol & Dhariwal, 2021) for diffusion model noise scheduling. Inspired by these advances, our work introduces a novel modification of the DiT architecture and flow matching for procedural activity learning, that leverages pretrained visual features on single video clips and explicitly models the temporal order of steps.

Procedural Activity Learning with Diffusion Models. Prior work has incorporated diffusion into procedural learning in various ways. Some works (Soucek et al., 2024; Black et al., 2024) propose using image- and text-conditioned diffusion-based generation or editing models to generate images of actions and object state changes while preserving the input image scene. These methods primarily use diffusion models as off-the-shelf tools for generating intermediate steps in the pixel space. In contrast, other works (Fang et al., 2023; Shi et al., 2025; Wang et al., 2023b; Zhong et al., 2023) integrate diffusion as a training objective within their model design, predicting the embeddings of unseen target clips based on the embeddings of observed clips. Our work follows this second approach, treating diffusion (flow matching) as a noise scheduler that denoises video embeddings from random noise, and we have designed a procedural learning framework based on the latest DiT architecture. Our framework differs from previous works in three folds: **(1) training supervision:** our model is designed to be trained directly with cross-entropy loss on downstream tasks, without the need for extra language supervision; **(2) prediction model architecture:** instead of using vanilla transformer blocks as the denoising model, we introduce a new Vector Embedding DiT architecture for procedural learning from videos, which is proved to be more effective; **(3) latent embedding generation:** Our model generates unseen video embeddings from a frozen encoder, thereby operating in the latent embedding space.

3 APPROACH

In this work, we look at three canonical tasks from the procedural representation learning literature, *Step forecasting*, *Procedure Planning*, and *Task classification*, following the setup from Zhong et al.

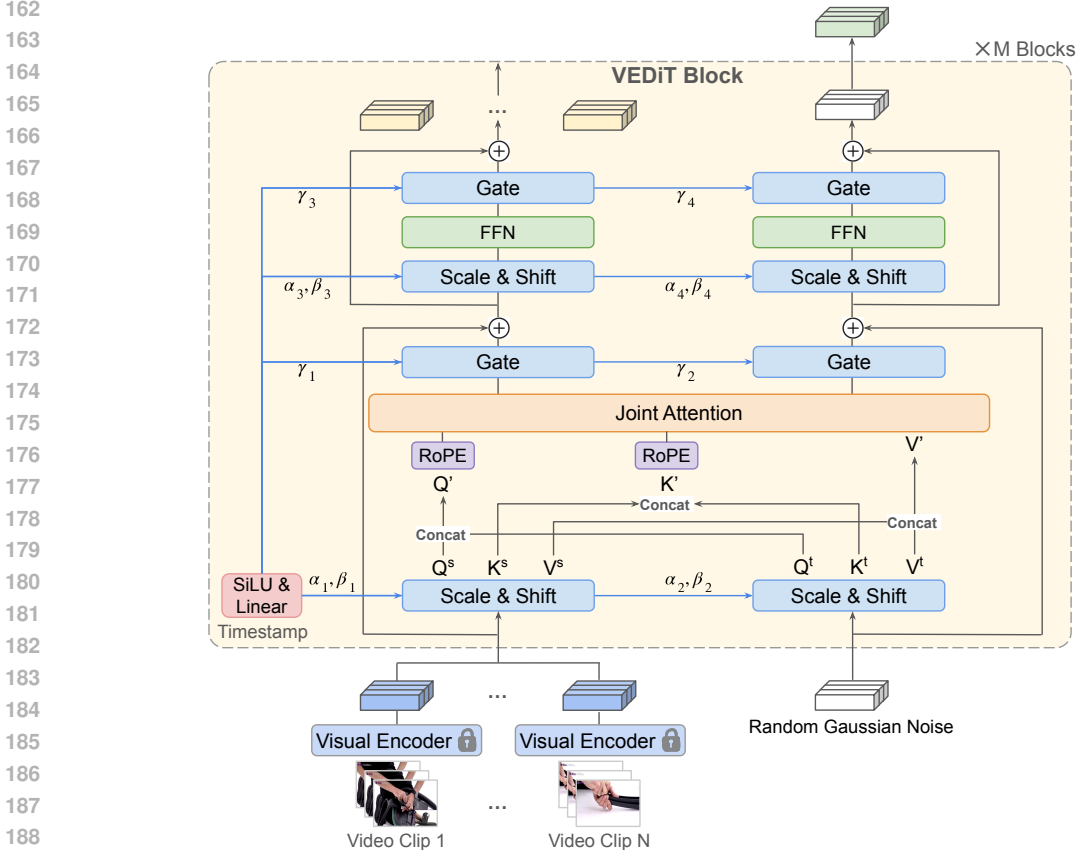


Figure 2: **Vector Embedding Diffusion Transformer (VEDiT) architecture.** During training, our model first uses frozen visual encoders to convert observed video clips into corresponding video embeddings. Then random Gaussian noises are generated as the initial video embeddings of unseen target clips. The DiT-based prediction model processes both seen and target video embeddings in two separate branches, and fuses their information via joint attention blocks where $Q' = \text{Concat}[Q^s, Q^t]$, $K' = \text{Concat}[K^s, K^t]$, $V' = \text{Concat}[V^s, V^t]$. To enable temporal modeling of clips, Rotary positional embeddings (RoPE) is applied to Q' and K' before being input to the attention module. The denoised target clip embeddings are then given as input to the attentive classifier in downstream tasks.

(2023); Niu et al. (2024). Given a series of video clips (or states) from a procedural event (i.e. cooking a dish), the objective is to a) predict the label of the unseen future event (or state) to occur (step forecasting), b) predict the label of unseen events that happened in-between (procedure planning) and c) predict the label of the entire set of events, from a list of probable classes (task classification). Generally, given a sequence of N observable video clip representations (v_i), we aim to learn a procedural state representation \hat{v} , which can either capture the information of unseen clips (step forecasting or procedure planning) or a summary information of the task (task classification) using a conditional predictor $\hat{v} = \mathcal{F}_\theta(\{v_i | i \in \mathcal{S}\})$, where \mathcal{S} is a set of observable clips. Using this representation, we then aim to learn a classifier to predict the class labels (\mathcal{C}) for the given task $h : \mathbb{R}^{k \times D} \rightarrow \mathcal{C}$, where k denotes a set of output embeddings for representation \hat{v} of dimension D .

Learning a predictor to predict an unseen clip representation typically requires an extensive training process to learn a rich visual representation *and* temporal information. In this work, we bypass the need of learning visual information by leveraging existing pre-trained encoders $v_i = \tau^*(v_i) \in \mathbb{R}^{k \times D}$, where v_i being the clip in pixel space. Therefore, we focus on learning the temporal transition among clips by operating over the encoder embeddings, $\hat{v} = \mathcal{F}_\theta(\{\tau^*(v_i) | i \in \mathcal{S}\})$, where the predictor needs to generate latent representation $\mathbb{R}^{k \times D}$ embeddings. To generate embeddings with rich visual signals, we draw inspiration from the diffusion model literature, particularly recent diffusion transformers (DiT) (Peebles & Xie, 2023; Esser et al., 2024). Given their powerful text-conditioned image and video generation capabilities (Yang et al., 2024; Ma et al., 2024a), we adapt their strong conditional generation architecture into a sequential step prediction model for procedural activities. Thus, learning

a strong predictor would allow us to generate *unseen* clip embeddings, to enable us to perform the tasks in procedural representation learning.

3.1 PRELIMINARY: LATENT DIFFUSION MODEL AND RECTIFIED FLOWS

Given an image $\mathbf{x} \in \mathbb{R}^{3 \times H \times W}$ with caption \mathbf{c} , image Latent diffusion models (LDMs) (Rombach et al., 2022) first use an autoencoder \mathcal{E} to encode the image into latents $\mathbf{z}_0 = \mathcal{E}(\mathbf{x}) \in \mathbb{R}^{C \times H' \times W'}$, where C represents the number of latent channels, and $H' = H/p$, $W' = W/p$ represent the spatial dimension of the latents, with p denotes as patch size. The forward diffusion process is a fixed diffusion process which adds random noise to the latent variable \mathbf{z}_0 . For example, forward process with Rectified Flows (RFs) (Liu et al., 2023; Lipman et al., 2023; Albergo & Vanden-Eijnden, 2023) is defined as a straight path between the data distribution \mathbf{z}_0 and a standard normal distribution ϵ (i.e., $\mathbf{z}_t = (1 - t)\mathbf{z}_0 + t\epsilon$, where $t \in [0, 1]$). The reverse process in RFs, on the other hand, gradually produces less noise samples starting from \mathbf{z}_1 to \mathbf{z}_0 in T denoising steps through a learnable transformer-based denoiser model \mathcal{F}_θ parameterized by θ and conditioned on caption \mathbf{c} . In our setup, we transform such denoiser model conditioned on caption/text into a sequential step prediction model for procedural activities conditioned on observed video clips, with explicit temporal order modeling via RoPE (Su et al., 2024).

3.2 OUR APPROACH: VECTOR EMBEDDING DIFFUSION TRANSFORMERS (VEDiT)

Overall Training Pipeline of VEDiT. The overall training pipeline of our VEDiT is illustrated in Fig. 1 left. Given a set \mathcal{S} that contains N observable (seen) video clips $\{v_1, v_2, \dots, v_N\}$, where each video clip $v_i \in \mathbb{R}^{K \times 3 \times H \times W}$ contains K frames, we first apply a frozen visual encoder $\tau^*(\cdot)$ to derive the corresponding video embeddings for each clip $v_i = \tau^*(v_i)$. Next, random Gaussian noises are generated as the initial video embeddings of unseen clips $\{\tilde{v}_j | j \in \mathcal{T}\}$, where \mathcal{T} represents the target set. Then we design VEDiT as the learnable prediction model \mathcal{F}_θ which predicts the unseen target video clip embeddings (\hat{v}) conditioned on all seen video embeddings: $\hat{v}_j = \mathcal{F}_\theta(\{v\}_i, \tilde{v}_j), i \in \mathcal{S}; j \in \mathcal{T}$. This prediction model is then trained using iterative denoising (Ho et al., 2020) over T steps, with diffusion timestamps sampled from the Flow Matching Euler Discrete Scheduler (Esser et al., 2024). Unlike DiT, which is based-on pixel-level and text-conditioned generation, our model is designed to predict abstract video features in the procedural activity, based on observed video clips. Additionally, unlike previous works (Lin et al., 2022; Zhong et al., 2023) for procedural activity understanding, our method does not use extra language supervision such as ASR or textual knowledge base (e.g., wikiHow) that aligns visual embeddings with text.

Training Objective of VEDiT. A key innovation and distinction of our method, compared with previous approaches to video embedding prediction for downstream tasks (Zhong et al., 2023; Lin et al., 2022)—which typically rely on a combination of multiple loss functions (such as video embedding reconstruction loss and video-language matching loss) for supervision—is that our pipeline can be effectively trained with a single cross-entropy loss. Unlike previous works that enforce alignment of the predicted video embeddings with often noisily annotated language descriptions, using a single cross-entropy loss allows the optimization target to align more effectively with downstream datasets.

Choice of Visual Encoder. Previous works on procedural learning (Lin et al., 2022; Zhong et al., 2023; Niu et al., 2024) typically use clip-level features as abstracted visual representation for each video clip, which can result in a loss of detail. Conversely, DiT models for image and video generation (Yang et al., 2024; Esser et al., 2024; Peebles & Xie, 2023) are designed for patch-level generation with a focus on fine-grained visual details, but this comes at the cost of higher computational demands. To ensure that our model can process videos with multiple clips, encode sufficient visual information, and avoid excessive computational costs, we explore our model with diverse CLIP- and SSL-based encoders that output visual features at the clip-, frame-, and patch-levels. We found empirically that using the [CLS] tokens of SigLIP (Zhai et al., 2023) from 16 uniformly sampled frames in each clip stands out as the strongest visual representation. An ablation study of visual encoders is discussed in Sec. 4.3.

VEDiT Model Architecture Design. Fig. 2 visualizes the components of each VEDiT block. Our architecture is derived from DiT (Peebles & Xie, 2023), which has a two-branch architecture with one *query* branch (typically text) tasked to condition the *target* branch (vision) through adaptive

layernorm (Perez et al., 2018). In our work, we utilize the *query* branch to process the observable (or seen) video encoder embeddings $\{v_i | i \in \mathcal{S}\}$, which conditions the *target* branch that operates on unseen, noisy embeddings $\{\tilde{v}_j | j \in \mathcal{T}\}$ through adaptive layernorm, which gets iteratively updated through denoising. The query branch is further conditioned by using the timestamp $t \in T$ sampled from the noise scheduler, along with its usual application of determining the scale of noise. Unlike DiT, the information of the query branch and the target branch are fused together using joint attention before being processed independently through feed-forward layers without weight sharing. Lastly, to enable temporal modeling of clips, Rotary positional embeddings (RoPE) (Su et al., 2024) is applied to the input immediately prior to the joint attention module. By utilizing these mechanisms, VEDiT allows us to learn unseen video embeddings, starting from noise, by conditioning on the observed video encoder representations. More ablations on design choices are provided in Appendix A.2.

4 EXPERIMENTS

In this section, we first introduce the evaluation datasets and the implementation details of our model in Sec. 4.1. We then compare our method with SOTAs on five downstream tasks across four datasets in Sec. 4.2. Finally, we present ablation studies on the visual encoders, as well as the necessity of pretraining on video clip sequences in Sec. 4.3. More ablations on VEDiT architecture design is provided in Appendix A.2.

4.1 EXPERIMENTAL SETUP

Evaluation Tasks and Datasets. We evaluate our method on five downstream tasks across four datasets. COIN (Tang et al., 2019) contains 476 hours of YouTube videos covering 180 tasks and 778 unique steps of daily activities. Following (Zhong et al., 2023; Lin et al., 2022), we evaluated our model on two tasks: step forecasting and task classification (see Fig. 1 for details). For Ego4D-v2 (Grauman et al., 2022), we focus on the long-term action anticipation benchmark, which aims to predict the next $Z = N - t$ future action classes [(verb₁, noun₁), (verb₂, noun₂), ..., (verb_Z, noun_Z)] given an input video up to timestamp t . This forecasting benchmark contains 243 hours of videos with a total of 3472 annotated clips. In addition, we utilize NIV (Alayrac et al., 2016), CrossTask (Zhukov et al., 2019), and COIN datasets to evaluate the procedure planning task (Chang et al., 2020), which can be seen as a variant of step forecasting task that aims at predicting intermediate action steps given the observed start and goal video clips. Specifically, CrossTask dataset contains 2750 videos covering 18 tasks and 133 actions, and NIV dataset contains 150 videos with 5 tasks and 48 actions. Following (Niu et al., 2024), we report the results with prediction horizon $T \in \{3, 4\}$.

Evaluation Metrics. For COIN step forecasting and task classification tasks, we use top-1 classification accuracy of the predicted step/task as the evaluation metric following DistantSup (Lin et al., 2022). For Ego4D-v2 long-horizon anticipation task, we use the default edit distance (ED) metric, which is computed as the Damerau-Levenshtein distance (Damerau, 1964) over sequences of predicted verbs or nouns. Following (Grauman et al., 2022), we report the minimum edit distance at $Z = 20$ (ED@20) for $K = 5$ predicted sequences on the validation set. In addition, for procedure planning tasks on NIV, CrossTask, and COIN, we evaluate the models on three metrics, including success rate (SR), mean Accuracy (mAcc) and mean Intersection over Union (mIoU) following previous works (Chang et al., 2020; Niu et al., 2024; Zhao et al., 2022).

Implementation Details. Our default VEDiT architecture contains 12 transformer blocks, with a hidden size of 2048 and attention head dimension of 64. During training, we apply classifier-free guidance with a scale of 7 and denoise the diffusion model for 24 steps using the Flow Matching Euler Discrete Scheduler (Esser et al., 2024). For COIN step forecasting and task classification tasks, we use a scheduled learning rate linearly increases from 5×10^{-6} to 5×10^{-5} during the first 3 epochs, and then decays to 5×10^{-7} following a cosine schedule, with a total of 30 epochs. For long-horizon anticipation and the procedure planning tasks, following the same training setting in previous works (Grauman et al., 2022; Niu et al., 2024), we train the model for 100 and 500 epochs respectively. Together with VEDiT, we train task specific attentive classifiers $h : \mathbb{R}^{k \times D} \rightarrow C$ (Bardes et al., 2024), which is an attentive pooler over k output embeddings followed by a single linear layer.

Model	Pretraining Supervision	Pretrain Data	Step Forecasting	Task Classification
Random Guess	N/A	N/A	0.1	-
SlowFast (Feichtenhofer et al., 2019)	Supervised: action labels	Kinetics	25.6	71.6
S3D (Xie et al., 2018)	Unsupervised: ASR w. MIL-NCE	HT100M	28.1	70.2
ClipBERT (Lei et al., 2021)	Supervised: captions	COCO+VG	-	65.4
VideoCLIP (Xu et al., 2021)	Unsupervised: ASR	HT100M	-	72.5
TSN (RGB + Flow) (Tang et al., 2019)	Supervised: action labels	Kinetics	-	73.4
TimeSformer (Bertasius et al., 2021)	Supervised: action labels	Kinetics	34.7	83.5
TimeSformer (Bertasius et al., 2021)	Unsupervised: ASR w. MIL-NCE	HT100M	34.0	85.3
DistantSup (Lin et al., 2022)	Unsupervised: ASR + wikiHow	HT100M	39.4	88.9
ProceduralVRL (Zhong et al., 2023)	Unsupervised: ASR	HT100M	46.8	90.8
Ours: TimeSformer + VEDiT	N/A	N/A	48.7	91.1
Ours: SigLIP (Zhai et al., 2023) + VEDiT	N/A	N/A	51.8	94.6

Table 1: Step forecasting and task classification results on COIN (Tang et al., 2019) dataset. We compare our method with a set of strong baselines as well as SOTA methods. Top-1 accuracies are reported. We **bold** and underline the best and the second best models in each task respectively.

4.2 MAIN RESULTS

Step Forecasting and Task Classification. In Table 1, we demonstrate the effectiveness of our VEDiT design on the COIN step forecasting and task classification tasks. Firstly, we use the pre-trained TimeSformer (Bertasius et al., 2021) visual encoder as τ^* , as used in ProceduralVRL (Zhong et al., 2023), the previous state-of-the-art in these tasks. We combined the TimeSformer encoder with VEDiT designed with joint attention, to arrive at the model TimeSformer+VEDiT. This model achieves improvements of 2.2% and 0.6% in top-1 accuracy on the step forecasting and task classification tasks. Next, using SigLIP (Zhai et al., 2023) as τ^* with VEDiT yields additional gains of 3.1% and 3.2% on these two tasks. It is worth noting our methods *does not require any large-scale pretraining on video clip sequences*, which proves the effectiveness of using strong language-aligned *single-clip pretrained* representations. Additionally, our method *does not require explicit text supervision* (i.e., unsupervised) compared to baselines DistantSup and ProceduralVRL, which are trained with explicit language matching loss (i.e., ASR or ASR+wikiHow). Furthermore, we observe linear *scalability* of VEDiT on Step Forecasting task, leading to improved numbers with increasing number of model parameters (Appendix A.2.3).

Procedure Planning Task. We further evaluate VEDiT on procedure planning results on the NIV, COIN, and CrossTask datasets with horizons $T \in \{3, 4\}$ in Table 2. Specifically, we build upon the previous SoTA model, SCHEMA (Niu et al., 2024), by replacing their vanilla transformer blocks in the state decoder and step decoder with our VEDiT blocks. To ensure a fair comparison, we use the same number of transformer blocks (i.e., 2 blocks) with identical hidden dimensions, attention heads, and we strictly adhere to their training and evaluation hyperparameters and setups without any changes. We report the mean and standard deviation of SR, mAcc, and mIoU for our results as well as our replication of SCHEMA averaged over 10 runs.

As shown in Table 2, SCHEMA with VEDiT consistently outperforms the original SCHEMA method on NIV (gains of 0.97%-2.28% for SR, 1.92%-3.39% for mAcc, and 0.49%-0.90% for mIoU) and COIN (gains of 2.21%-5.89% for SR, 2.31%-7.07% for mAcc, and 0.86%-2.57% for mIoU). Additionally, our VEDiT achieves better average performance on the CrossTask dataset. Moreover, as plotted in Fig. 3, we also observe better stability of VEDiT over vanilla transformer blocks as we scale up the number of transformer blocks.

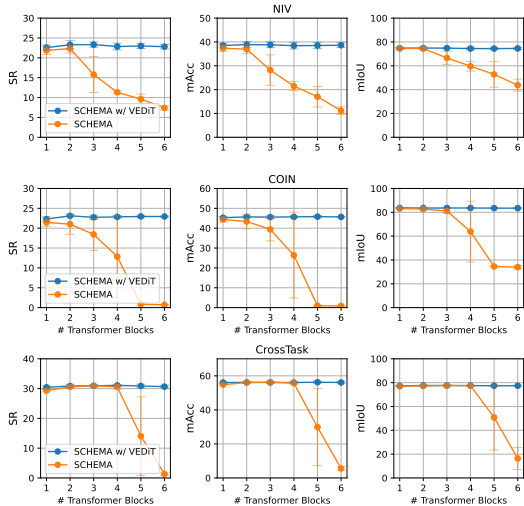


Figure 3: SCHEMA w/ VEDiT is more stable than SCHEMA w/ vanilla transformer as we increase the number of transformer blocks.

378
379
380
381
382
383
384
385
386
387
388
389
390
391
392
393
394
395
396
397
398
399
400
401
402
403
404
405
406
407

Datasets	Models	$T = 3$			$T = 4$		
		SR (\uparrow)	mAcc (\uparrow)	mIoU (\uparrow)	SR (\uparrow)	mAcc (\uparrow)	mIoU (\uparrow)
NIV	Random	2.21	4.07	6.09	1.12	2.73	5.84
	DDN (Chang et al., 2020)	18.41	32.54	56.56	15.97	27.09	53.84
	Ext-GAIL (Bi et al., 2021)	22.11	42.20	65.93	19.91	36.31	53.84
	P ³ IV (Zhao et al., 2022)	24.68	49.01	74.29	20.14	38.36	67.29
	EGPP (Wang et al., 2023a)	26.05	51.24	75.81	21.37	41.96	74.90
	SCHEMA (Niu et al., 2024)	27.93	41.64	76.77	23.26	39.93	76.75
	SCHEMA [†]	26.66 \pm 2.27	39.94 \pm 2.79	75.58 \pm 1.47	22.32 \pm 1.15	36.96 \pm 1.84	74.39 \pm 1.13
	SCHEMA w/ VEDiT (Ours)	28.94\pm1.07 (2.28 \uparrow)	43.33\pm0.90 (3.39 \uparrow)	76.48\pm0.62 (0.90 \uparrow)	23.29\pm0.44 (0.97 \uparrow)	38.88\pm1.19 (1.92 \uparrow)	74.88\pm0.89 (0.49 \uparrow)
	Random	<0.01	<0.01	2.47	< 0.01	< 0.01	2.32
	Retrieval	4.38	17.40	32.06	2.71	14.29	36.97
COIN	DDN (Chang et al., 2020)	13.90	20.19	64.78	11.13	17.71	68.06
	P ³ IV (Zhao et al., 2022)	15.40	21.67	76.31	11.32	18.85	70.53
	EGPP (Wang et al., 2023a)	19.57	31.42	84.95	13.59	26.72	84.72
	SCHEMA (Niu et al., 2024)	32.09	49.84	83.83	22.02	45.33	83.47
	SCHEMA [†]	26.38 \pm 3.66	43.08 \pm 4.28	81.49 \pm 1.70	21.00 \pm 2.56	43.37 \pm 3.64	82.70 \pm 1.08
	SCHEMA w/ VEDiT (Ours)	32.27\pm0.44 (5.89 \uparrow)	50.15\pm0.31 (7.07 \uparrow)	84.07 \pm 0.38 (2.57 \uparrow)	23.11\pm0.27 (2.11 \uparrow)	45.68\pm0.52 (2.31 \uparrow)	83.56 \pm 0.45 (0.86 \uparrow)
	Random	<0.01	0.94	1.66	< 0.01	0.83	1.66
	Retrieval	8.05	23.30	32.06	3.95	22.22	36.97
	DDN (Chang et al., 2020)	12.18	31.29	47.48	5.97	27.10	48.46
	Ext-GAIL (Bi et al., 2021)	21.27	49.46	61.70	16.41	43.05	60.93
CrossTask	P ³ IV (Zhao et al., 2022)	23.34	49.96	73.89	13.40	44.16	70.01
	PPDP (Wang et al., 2023b)	26.38	55.62	59.34	18.69	52.44	62.38
	EGPP (Wang et al., 2023a)	26.40	53.02	74.05	16.49	48.00	70.16
	SCHEMA (Niu et al., 2024)	31.83	57.31	78.33	19.71	51.85	74.46
	SCHEMA [†]	30.57 \pm 0.38	56.02 \pm 0.32	77.60\pm0.25	20.26 \pm 0.33	51.93 \pm 0.17	74.51 \pm 0.25
	SCHEMA w/ VEDiT (Ours)	31.08\pm0.31 (0.51 \uparrow)	56.15\pm0.57 (0.13 \uparrow)	77.54 \pm 0.35 (0.06 \downarrow)	20.42\pm0.24 (0.16 \uparrow)	52.26 \pm 0.51 (0.33 \uparrow)	74.76\pm0.29 (0.25 \uparrow)

Table 2: Procedure planning results on NIV (Alayrac et al., 2016), COIN (Tang et al., 2019), and CrossTask (Zhukov et al., 2019) datasets with prediction horizon $T \in \{3, 4\}$. SCHEMA[†]: our replication of their method averaged over 10 runs. The best numbers are **bolded**. Our improvement over SCHEMA baseline is colored in **blue**.

408
409
410
411
412

Method	Encoder	Prediction Model	ED@5 (\downarrow)		ED@20 (\downarrow)	
			Verb	Noun	Verb	Noun
Ego4D Baseline (Grauman et al., 2022)	SlowFast	Transformer	-	-	0.745	0.779
Ego4D Baseline (Grauman et al., 2022)	SigLIP	Transformer	0.703	0.736	0.718	0.742
PaMsEgoAI (Ishibashi et al., 2023)	SlowFast + CLIP	Concat + Transformer	-	-	0.670	0.629
Ours	SigLIP	VEDiT	0.677	0.711	0.697	0.711

413
414
415
416
417
418
419
420
421
422
423
424
425
426
427
428
429
430
431

Table 3: Comparison of methods on the validation set of Ego4D (Grauman et al., 2022) long-term action anticipation challenge. Edit distance (ED) metrics are reported at prediction horizon 5 and 20.

Long-Horizon Action Anticipation. In Table 3, we evaluate our model on the Ego4D-v2 long-horizon action anticipation task. We introduce a new baseline by replacing the SlowFast (Feichtenhofner et al., 2019) visual encoder in the Ego4D baseline model with SigLIP, while keeping the prediction model (*i.e.*, `slowfast_trf_v2`) unchanged. For a fair comparison, we initialize VEDiT with the same number of transformer blocks and hidden dimension size as the Ego4D baseline transformer prediction model. Using SigLIP as visual encoder, VEDiT outperforms the Ego4D baseline in both Verb ED@20 (Ours: 0.697 v.s. Ego4D Baseline: 0.718, lower is better) and noun ED@20 (Ours: 0.711 v.s. Ego4D Baseline: 0.742, lower is better). In addition, while not directly comparable, PaMsEgoAI (Ishibashi et al., 2023), achieves lower ED metrics by introducing several enhancements, including an ensemble of SlowFast and SlowFast-CLIP models, label smoothing to relax order constraints for future actions, and constraining the (verb, noun) classes based on word co-occurrence. Some studies (Zhao et al., 2024; Pei et al., 2024; Huang et al., 2023) have found that combining vision models with the strong planning capabilities of LLMs can achieve good performance, particularly for long-horizon action anticipation tasks. Therefore, integrating our method with an LLM could be a promising future direction.

Model	Architecture	Pretrain Data	CLIP/SSL	Token	Step Forecasting	Task Classification
DINOv2	ViT-Giant/14@224	LVD-142M (Oquab et al., 2024)	SSL	[CLS]	47.03	<u>90.89</u>
VJEPa	ViT-Huge/16@224	VideoMix2M (Bardes et al., 2024)	SSL	Patch	47.24	86.13
VJEPa	ViT-Huge/16@384	VideoMix2M (Bardes et al., 2024)	SSL	Patch	<u>48.23</u>	87.14
VideoMAE	ViT-Huge/16@224	K400 (Kay et al., 2017)	SSL	Patch	44.78	83.40
SigLIP (default)	ViT-SO400M/14@384	WebLI (Chen et al., 2023)	CLIP	[CLS]	50.05	94.38

Table 4: Ablation on frozen video encoders on COIN (Tang et al., 2019) step forecasting and procedural activity classification tasks. Top-1 accuracies are reported. We **bold** and underline the best and the second best models in each task respectively.

4.3 ABLATIONS

4.3.1 WHICH VISUAL ENCODER WORKS BEST?

To test the impact of visual encoders on procedural activity understanding from instructional videos, we train VEDiT with 3 blocks for 10 epochs with different visual encoders. We include strong CLIP-based and self-supervised (SSL) encoders, including SigLIP (ViT-SO400M/14@384) (Zhai et al., 2023), V-JEPa (Bardes et al., 2024), DINOv2 (Oquab et al., 2024), and VideoMAE Tong et al. (2022). For V-JEPa and VideoMAE, we provide patch tokens to VEDiT, while for DINOv2 and SigLIP, we provide [CLS] tokens. We evaluate the model trained with different encoders on COIN for step forecasting and task classification tasks.

As we observe from Table 4, SigLIP outperforms SSL-based encoders. Among the SSL-based encoders, VJEPa ViT-H 384 and DINOv2 performs comparably than the baselines for step forecasting and task classification task respectively. SigLIP outperforms both on a large margin, especially in Task classification, highlighting the need of language-aligned rich visual representations for stronger procedural activity understanding.

4.3.2 IS PRE-TRAINING NECESSARY?

Instead of training directly on downstream datasets (*i.e.*, COIN), previous works (Zhong et al., 2023; Lin et al., 2022) undergo large-scale [pretraining on video clip sequences](#) from publicly available video datasets, such as HowTo100M (Miech et al., 2019). In this section, we question whether such [clip-sequence pretraining](#) is necessary. Specifically, we compare our model trained directly on COIN with a variant that includes additional [clip-sequence pretraining](#) on HowTo100M dataset. Following the recipe of Zhong et al. (2023), we set the total number of clips to 9, randomly mask out the video embedding of one clip, and use the masked clip embedding reconstruction as the training objective. Additionally, instead of relying on the noisy automatic speech recognition (ASR) annotations, we use the starting and ending timestamps of each video clip processed and filtered by HowToCaption (Shvetsova et al., 2024). During pretraining, we employ the AdamW (Loshchilov & Hutter, 2019) optimizer, with the learning rate linearly increasing from 1×10^{-5} to 1×10^{-4} during the first 0.5 training epochs, and then remaining constant for a total of 30 epochs. The pretraining is conducted on 128 H100 GPUs with a total batch size of 1024, and takes 2 days and 4.5 days for the 165M and 1.77B VEDiT models respectively (see Table 8 for model architecture details).

Surprisingly, we observe only marginal improvement with significant [clip-sequence pretraining](#) (Table 5). [Pretraining on video clip sequences](#) only provides an additional 0.3% boost in top-1 accuracy for the step forecasting task. We hypothesize this limited effectiveness of [clip-sequence pretraining](#) may stem from two factors: (1) pretraining dataset is relatively noisy, leading to a distribution gap with the downstream COIN dataset, and (2) the pretraining objective in (Zhong et al., 2023) may not be optimal. Exploring better [clip-sequence pretraining](#) objectives that can generalize well across different downstream tasks is left for future work.

5 LIMITATIONS

One potential limitation of our model with multi-step denoising is that it sacrifices efficiency for performance. Additionally, it is not specifically designed for real-time inference, which is a parallel topic to our paper and typically involves techniques such as model distillation, quantization, and hardware-level optimization. We leave the exploration of this direction for future work.

Model	Pretraining Supervision	Pretrain Data	Step Forecasting	Task Classification
SigLIP + VEDiT	N/A	N/A	51.8	94.6
SigLIP + VEDiT	Unsupervised: HowToCaption	HT100M	52.1	94.6

Table 5: Effect of large-scale [clip-sequence pretraining](#). We compare VEDiT without large-scale pretraining with a variant that’s pretrained on 1.16M videos from HowTo100M (Miech et al., 2019) dataset, using temporal information from HowToCaption (Shvetsova et al., 2024). Top-1 accuracies are reported.

# Denoising Steps	1	4	8	12	16	20	24
Training Clock Time (sec.)	0.41	0.49	0.63	0.82	0.94	1.09	1.24
Inference Clock Time (sec.)	0.40	0.47	0.56	0.66	0.75	0.84	0.93
Training GPU Memory (GB)	21.8	21.9	22.0	22.0	22.1	22.2	22.3
Inference GPU Memory (GB)	15.7	15.7	15.8	15.8	15.8	15.8	15.9

Table 6: Training and inference clock time and GPU memory of VEDiT as we increase the number of denoising steps.

Here, we provide some analysis by evaluating the training and inference time as well as GPU memory usage of our model with varying numbers of denoising steps. Specifically, we conducted this experiment using the VEDiT architecture with 696M trainable parameters. We measured the clock time and GPU memory required to run inference on the model using 1 COIN video consisting of 8 clips, with gradient checkpointing enabled.

As shown in the table below, increasing the number of denoising steps from 1 to 24 results in only a $1.32\times$ increase in inference time and a $2.02\times$ increase in training time. This efficiency is partially because of the adoption of efficient scalable dot product attention in each VEDiT block. Moreover, because we employ gradient checkpointing to optimize GPU memory usage, GPU memory usage remains nearly constant without significant variation.

6 CONCLUSION

In this work, we demonstrate that carefully designed predictive models learned on top of [single-clip pretrained](#) visual representations can achieve state-of-the-art performance on procedural learning tasks across the COIN, CrossTask, NIV, and Ego4D datasets, including step forecasting, procedural activity classification, procedure planning, and long-term action anticipation. Notably, we achieve these results without pretraining the prediction module, instead learning it directly from the end tasks. This contrasts with previous works, which often require computationally expensive pretraining of the predictor, sometimes with additional supervision. Our findings suggest that further research is needed to improve [clip-sequence pretraining](#) for procedural activities. Specifically, exploring ways to better align pretraining tasks with downstream tasks could help fully leverage the benefits of pretraining. Moreover, the data distribution gap, as well as differences in the timestep boundaries of clips between the large-scale pretraining dataset and the downstream dataset, could be a potential bottleneck that hinders the effectiveness of large-scale pretraining on noisy videos. Strategies aimed at improving robustness to distribution shifts (Sun et al., 2020) represent another promising direction for exploration.

7 REPRODUCIBILITY

In this work, we aim to make VEDiT training and evaluation reproducible, so that readers can assimilate the contributions in their own work. By design, VEDiT is highly reproducible as it doesn’t require expensive pre-training, as it works on top of frozen vision encoders, specifically SigLIP¹ for our main experiments. We ground the discussion of model development in Sec. 3.2. We provide details of the training pipeline, training & evaluation data and metrics used in Sec. 4.1. Further results on step classification task and procedure planning tasks are provided in Appendix A.1 for assiting

¹<https://huggingface.co/google/siglip-so400m-patch14-384>

540 replicability and generalization of VEDiT. Detailed ablation results on the model design, including
 541 choice of attention mechanism and denoising steps, are provided in Appendix A.2.3. Finally, we
 542 provide detailed results on the scalability of VEDiT to further shed light on its generalizability with
 543 increasing amount of model parameters. PyTorch (Ansel et al., 2024) implementation of VEDiT
 544 blocks is provided in Algorithm 1. We will release our code post peer review.

546 REFERENCES

- 547 Triantafyllos Afouras, Effrosyni Mavroudi, Tushar Nagarajan, Huiyu Wang, and Lorenzo Torresani.
 548 Ht-step: Aligning instructional articles with how-to videos. *Advances in Neural Information*
 549 *Processing Systems*, 36, 2024.
- 551 Jean-Baptiste Alayrac, Piotr Bojanowski, Nishant Agrawal, Josef Sivic, Ivan Laptev, and Simon
 552 Lacoste-Julien. Unsupervised learning from narrated instruction videos. In *Proceedings of the*
 553 *IEEE conference on computer vision and pattern recognition*, pp. 4575–4583, 2016.
- 554 Michael Samuel Albergo and Eric Vanden-Eijnden. Building normalizing flows with stochastic
 555 interpolants. In *The Eleventh International Conference on Learning Representations*, 2023.
- 557 Jason Ansel, Edward Yang, Horace He, Natalia Gimelshein, Animesh Jain, Michael Voznesensky,
 558 Bin Bao, Peter Bell, David Berard, Evgeni Burovski, Geeta Chauhan, Anjali Chourdia, Will
 559 Constable, Alban Desmaison, Zachary DeVito, Elias Ellison, Will Feng, Jiong Gong, Michael
 560 Gschwind, Brian Hirsh, Sherlock Huang, Kshiteej Kalambarkar, Laurent Kirsch, Michael Lazos,
 561 Mario Lezcano, Yanbo Liang, Jason Liang, Yinghai Lu, CK Luk, Bert Maher, Yunjie Pan, Christian
 562 Puhersch, Matthias Reso, Mark Saroufim, Marcos Yukio Siraichi, Helen Suk, Michael Suo, Phil
 563 Tillet, Eikan Wang, Xiaodong Wang, William Wen, Shunting Zhang, Xu Zhao, Keren Zhou,
 564 Richard Zou, Ajit Mathews, Gregory Chanan, Peng Wu, and Soumith Chintala. PyTorch 2: Faster
 565 Machine Learning Through Dynamic Python Bytecode Transformation and Graph Compilation.
 566 In *29th ACM International Conference on Architectural Support for Programming Languages and*
 567 *Operating Systems, Volume 2 (ASPLOS '24)*. ACM, April 2024. doi: 10.1145/3620665.3640366.
 URL <https://pytorch.org/assets/pytorch2-2.pdf>.
- 568 Mahmoud Assran, Quentin Duval, Ishan Misra, Piotr Bojanowski, Pascal Vincent, Michael Rabbat,
 569 Yann LeCun, and Nicolas Ballas. Self-supervised learning from images with a joint-embedding
 570 predictive architecture. In *Proceedings of the IEEE/CVF Conference on Computer Vision and*
 571 *Pattern Recognition*, pp. 15619–15629, 2023.
- 572 Adrien Bardes, Quentin Garrido, Jean Ponce, Xinlei Chen, Michael Rabbat, Yann LeCun, Mido
 573 Assran, and Nicolas Ballas. Revisiting feature prediction for learning visual representations from
 574 video. *Transactions on Machine Learning Research*, 2024. ISSN 2835-8856. URL <https://openreview.net/forum?id=QaCCuDfBk2>. Featured Certification.
- 575 Gedas Bertasius, Heng Wang, and Lorenzo Torresani. Is space-time attention all you need for video
 576 understanding? In *Proceedings of the International Conference on Machine Learning (ICML)*,
 577 July 2021.
- 580 Jing Bi, Jiebo Luo, and Chenliang Xu. Procedure planning in instructional videos via contextual
 581 modeling and model-based policy learning. In *Proceedings of the IEEE/CVF International*
 582 *Conference on Computer Vision*, 2021.
- 583 Kevin Black, Mitsuhiko Nakamoto, Pranav Atreya, Homer Rich Walke, Chelsea Finn, Aviral Kumar,
 584 and Sergey Levine. Zero-shot robotic manipulation with pre-trained image-editing diffusion
 585 models. In *The Twelfth International Conference on Learning Representations*, 2024. URL
 586 <https://openreview.net/forum?id=c0chJTSbci>.
- 587 Andreas Blattmann, Robin Rombach, Huan Ling, Tim Dockhorn, Seung Wook Kim, Sanja Fidler, and
 588 Karsten Kreis. Align your latents: High-resolution video synthesis with latent diffusion models.
 589 In *Proceedings of the IEEE/CVF Conference on Computer Vision and Pattern Recognition*, pp.
 590 22563–22575, 2023.
- 591 Anthony Brohan, Yevgen Chebotar, Chelsea Finn, Karol Hausman, Alexander Herzog, Daniel Ho,
 592 Julian Ibarz, Alex Irpan, Eric Jang, Ryan Julian, et al. Do as i can, not as i say: Grounding language
 593 in robotic affordances. In *Conference on robot learning*, pp. 287–318. PMLR, 2023.

- 594 Chien-Yi Chang, De-An Huang, Danfei Xu, Ehsan Adeli, Li Fei-Fei, and Juan Carlos Niebles.
595 Procedure planning in instructional videos. In *European Conference on Computer Vision*, 2020.
596
- 597 Junsong Chen, YU Jincheng, GE Chongjian, Lewei Yao, Enze Xie, Zhongdao Wang, James Kwok,
598 Ping Luo, Huchuan Lu, and Zhenguo Li. Pixart- α : Fast training of diffusion transformer for
599 photorealistic text-to-image synthesis. In *The Twelfth International Conference on Learning*
600 *Representations*, 2024.
- 601 Xi Chen, Xiao Wang, Soravit Changpinyo, AJ Piergiovanni, Piotr Padlewski, Daniel Salz, Se-
602 bastian Goodman, Adam Grycner, Basil Mustafa, Lucas Beyer, Alexander Kolesnikov, Joan
603 Puigcerver, Nan Ding, Keran Rong, Hassan Akbari, Gaurav Mishra, Linting Xue, Ashish V
604 Thapliyal, James Bradbury, Weicheng Kuo, Mojtaba Seyedhosseini, Chao Jia, Burcu Karagol
605 Ayan, Carlos Riquelme Ruiz, Andreas Peter Steiner, Anelia Angelova, Xiaohua Zhai, Neil
606 Houlsby, and Radu Soricut. PaLI: A jointly-scaled multilingual language-image model. In
607 *The Eleventh International Conference on Learning Representations*, 2023. URL <https://openreview.net/forum?id=mWVoBz4W0u>.
608
- 609 Xinlei Chen, Hao Fang, Tsung-Yi Lin, Ramakrishna Vedantam, Saurabh Gupta, Piotr Dollár, and
610 C Lawrence Zitnick. Microsoft coco captions: Data collection and evaluation server. 2015.
611
- 612 Xinlei Chen, Saining Xie, and Kaiming He. An empirical study of training self-supervised vision
613 transformers. In *Proceedings of the IEEE/CVF international conference on computer vision*, pp.
614 9640–9649, 2021.
- 615 Fred J Damerau. A technique for computer detection and correction of spelling errors. *Communica-*
616 *tions of the ACM*, 7(3):171–176, 1964.
617
- 618 Patrick Esser, Sumith Kulal, Andreas Blattmann, Rahim Entezari, Jonas Müller, Harry Saini, Yam
619 Levi, Dominik Lorenz, Axel Sauer, Frederic Boesel, et al. Scaling rectified flow transformers for
620 high-resolution image synthesis. In *Forty-first International Conference on Machine Learning*,
621 2024.
- 622 Fen Fang, Yun Liu, Ali Koksul, Qianli Xu, and Joo-Hwee Lim. Masked diffusion with task-awareness
623 for procedure planning in instructional videos. *arXiv preprint arXiv:2309.07409*, 2023.
624
- 625 Christoph Feichtenhofer, Haoqi Fan, Jitendra Malik, and Kaiming He. Slowfast networks for video
626 recognition. In *Proceedings of the IEEE/CVF international conference on computer vision*, pp.
627 6202–6211, 2019.
- 628 Peng Gao, Le Zhuo, Ziyi Lin, Chris Liu, Junsong Chen, Ruoyi Du, Enze Xie, Xu Luo, Longtian Qiu,
629 Yuhang Zhang, et al. Lumina-t2x: Transforming text into any modality, resolution, and duration
630 via flow-based large diffusion transformers. *arXiv preprint arXiv:2405.05945*, 2024.
- 631 Ian Goodfellow, Yoshua Bengio, Aaron Courville, and Yoshua Bengio. *Deep learning*, volume 1.
632 MIT Press, 2016.
633
- 634 Kristen Grauman, Andrew Westbury, Eugene Byrne, Zachary Chavis, Antonino Furnari, Rohit
635 Girdhar, Jackson Hamburger, Hao Jiang, Miao Liu, Xingyu Liu, et al. Ego4d: Around the world in
636 3,000 hours of egocentric video. In *Proceedings of the IEEE/CVF Conference on Computer Vision*
637 *and Pattern Recognition*, pp. 1895–19012, 2022.
- 638 Kaiming He, Xinlei Chen, Saining Xie, Yanghao Li, Piotr Dollár, and Ross Girshick. Masked
639 autoencoders are scalable vision learners. In *Proceedings of the IEEE/CVF conference on computer*
640 *vision and pattern recognition*, pp. 16000–16009, 2022.
641
- 642 Jonathan Ho, Ajay Jain, and Pieter Abbeel. Denoising diffusion probabilistic models. *Advances in*
643 *neural information processing systems*, 33:6840–6851, 2020.
- 644 Daoji Huang, Otmar Hilliges, Luc Van Gool, and Xi Wang. Palm: Predicting actions through language
645 models @ ego4d long-term action anticipation challenge. *arXiv preprint arXiv:2306.16545*, 2023.
646
- 647 Tatsuya Ishibashi, Kosuke Ono, Noriyuki Kugo, and Yuji Sato. Technical report for ego4d long term
action anticipation challenge 2023, 2023. URL <https://arxiv.org/abs/2307.01467>.

- 648 Tero Karras, Miika Aittala, Timo Aila, and Samuli Laine. Elucidating the design space of diffusion-
649 based generative models. *Advances in neural information processing systems*, 35:26565–26577,
650 2022.
- 651 Will Kay, João Carreira, Karen Simonyan, Brian Zhang, Chloe Hillier, Sudheendra Vijayanarasimhan,
652 Fabio Viola, Tim Green, Trevor Back, Apostol Natsev, Mustafa Suleyman, and Andrew Zisserman.
653 The kinetics human action video dataset. *ArXiv*, abs/1705.06950, 2017.
- 654 Jacob Devlin Ming-Wei Chang Kenton and Lee Kristina Toutanova. Bert: Pre-training of deep
655 bidirectional transformers for language understanding. In *Proceedings of naacL-HLT*, volume 1,
656 pp. 2. Minneapolis, Minnesota, 2019.
- 657 Mahnaz Koupaee and William Yang Wang. Wikihow: A large scale text summarization dataset.
658 *arXiv preprint arXiv:1810.09305*, 2018.
- 659 Ranjay Krishna, Yuke Zhu, Oliver Groth, Justin Johnson, Kenji Hata, Joshua Kravitz, Stephanie
660 Chen, Yannis Kalantidis, Li-Jia Li, David A Shamma, et al. Visual genome: Connecting language
661 and vision using crowdsourced dense image annotations. *International journal of computer vision*,
662 123:32–73, 2017.
- 663 Yann LeCun. A path towards autonomous machine intelligence version 0.9. 2, 2022-06-27. *Open*
664 *Review*, 62(1):1–62, 2022.
- 665 Jie Lei, Linjie Li, Luowei Zhou, Zhe Gan, Tamara L Berg, Mohit Bansal, and Jingjing Liu. Less
666 is more: Clipbert for video-and-language learning via sparse sampling. In *Proceedings of the*
667 *IEEE/CVF conference on computer vision and pattern recognition*, pp. 7331–7341, 2021.
- 668 Xudong Lin, Fabio Petroni, Gedas Bertasius, Marcus Rohrbach, Shih-Fu Chang, and Lorenzo
669 Torresani. Learning to recognize procedural activities with distant supervision. In *Proceedings of*
670 *the IEEE/CVF Conference on Computer Vision and Pattern Recognition*, pp. 13853–13863, 2022.
- 671 Yaron Lipman, Ricky TQ Chen, Heli Ben-Hamu, Maximilian Nickel, and Matthew Le. Flow matching
672 for generative modeling. In *The Eleventh International Conference on Learning Representations*,
673 2023.
- 674 Xingchao Liu, Chengyue Gong, et al. Flow straight and fast: Learning to generate and transfer data
675 with rectified flow. In *The Eleventh International Conference on Learning Representations*, 2023.
- 676 Ilya Loshchilov and Frank Hutter. Decoupled weight decay regularization. In *International Confer-*
677 *ence on Learning Representations*, 2019.
- 678 Bingqi Ma, Zhuofan Zong, Guanglu Song, Hongsheng Li, and Yu Liu. Exploring the role of large
679 language models in prompt encoding for diffusion models. *arXiv preprint arXiv:2406.11831*,
680 2024a.
- 681 Nanye Ma, Mark Goldstein, Michael S Albergo, Nicholas M Boffi, Eric Vanden-Eijnden, and
682 Saining Xie. Sit: Exploring flow and diffusion-based generative models with scalable interpolant
683 transformers. *arXiv preprint arXiv:2401.08740*, 2024b.
- 684 Xin Ma, Yaohui Wang, Gengyun Jia, Xinyuan Chen, Ziwei Liu, Yuan-Fang Li, Cunjian Chen, and
685 Yu Qiao. Latte: Latent diffusion transformer for video generation. *arXiv preprint arXiv:2401.03048*,
686 2024c.
- 687 Antoine Miech, Dimitri Zhukov, Jean-Baptiste Alayrac, Makarand Tapaswi, Ivan Laptev, and Josef
688 Sivic. Howto100m: Learning a text-video embedding by watching hundred million narrated
689 video clips. In *Proceedings of the IEEE/CVF international conference on computer vision*, pp.
690 2630–2640, 2019.
- 691 Alexander Quinn Nichol and Prafulla Dhariwal. Improved denoising diffusion probabilistic models.
692 In *International conference on machine learning*, pp. 8162–8171. PMLR, 2021.
- 693 Yulei Niu, Wenliang Guo, Long Chen, Xudong Lin, and Shih-Fu Chang. SCHEMA: State CHanges
694 MAtter for procedure planning in instructional videos. In *The Twelfth International Conference on*
695 *Learning Representations*, 2024.

- 702 Maxime Oquab, Timothée Darcet, Théo Moutakanni, Huy Vo, Marc Szafraniec, Vasil Khalidov,
703 Pierre Fernandez, Daniel Haziza, Francisco Massa, Alaaeldin El-Nouby, et al. Dinov2: Learning
704 robust visual features without supervision. *Transactions on Machine Learning Research Journal*,
705 pp. 1–31, 2024.
- 706 William Peebles and Saining Xie. Scalable diffusion models with transformers. In *Proceedings of*
707 *the IEEE/CVF International Conference on Computer Vision*, pp. 4195–4205, 2023.
- 708
- 709 Baoqi Pei, Guo Chen, Jilan Xu, Yuping He, Yicheng Liu, Kanghua Pan, Yifei Huang, Yali Wang,
710 Tong Lu, Limin Wang, and Yu Qiao. Egovideo: Exploring egocentric foundation model and
711 downstream adaptation. *arXiv preprint arXiv:2406.18070*, 2024.
- 712
- 713 Ethan Perez, Florian Strub, Harm De Vries, Vincent Dumoulin, and Aaron Courville. Film: Visual
714 reasoning with a general conditioning layer. In *Proceedings of the AAAI conference on artificial*
715 *intelligence*, volume 32, 2018.
- 716 Alec Radford, Jong Wook Kim, Chris Hallacy, Aditya Ramesh, Gabriel Goh, Sandhini Agarwal,
717 Girish Sastry, Amanda Askell, Pamela Mishkin, Jack Clark, et al. Learning transferable visual
718 models from natural language supervision. In *International conference on machine learning*, pp.
719 8748–8763. PMLR, 2021.
- 720 Robin Rombach, Andreas Blattmann, Dominik Lorenz, Patrick Esser, and Björn Ommer. High-
721 resolution image synthesis with latent diffusion models. In *Proceedings of the IEEE/CVF confer-*
722 *ence on computer vision and pattern recognition*, pp. 10684–10695, 2022.
- 723
- 724 Fadime Sener, Dibyadip Chatterjee, Daniel Sheleпов, Kun He, Dipika Singhania, Robert Wang,
725 and Angela Yao. Assembly101: A large-scale multi-view video dataset for understanding proce-
726 dural activities. In *Proceedings of the IEEE/CVF Conference on Computer Vision and Pattern*
727 *Recognition*, pp. 21096–21106, 2022.
- 728 Lei Shi, Paul-Christian Bürkner, and Andreas Bulling. Actiondiffusion: An action-aware diffusion
729 model for procedure planning in instructional videos. In *Proc. IEEE/CVF Winter Conference on*
730 *Applications of Computer Vision (WACV)*, 2025.
- 731
- 732 Nina Shvetsova, Anna Kukleva, Xudong Hong, Christian Rupprecht, Bernt Schiele, and Hilde Kuehne.
733 Howtocation: Prompting llms to transform video annotations at scale. *ECCV*, 2024.
- 734
- 735 Jascha Sohl-Dickstein, Eric Weiss, Niru Maheswaranathan, and Surya Ganguli. Deep unsupervised
736 learning using nonequilibrium thermodynamics. In *International conference on machine learning*,
737 pp. 2256–2265. PMLR, 2015.
- 738
- 739 Jiaming Song, Chenlin Meng, and Stefano Ermon. Denoising diffusion implicit models. In *Interna-*
740 *tional Conference on Learning Representations*, 2020a.
- 741
- 742 Yale Song, Eugene Byrne, Tushar Nagarajan, Huiyu Wang, Miguel Martin, and Lorenzo Torresani.
743 Ego4d goal-step: Toward hierarchical understanding of procedural activities. *Advances in Neural*
744 *Information Processing Systems*, 36, 2024.
- 745
- 746 Yang Song, Jascha Sohl-Dickstein, Diederik P Kingma, Abhishek Kumar, Stefano Ermon, and Ben
747 Poole. Score-based generative modeling through stochastic differential equations. In *International*
748 *Conference on Learning Representations*, 2020b.
- 749
- 750 Tomas Soucek, Dima Damen, Michael Wray, Ivan Laptev, and Josef Sivic. Genhowto: Learning to
751 generate actions and state transformations from instructional videos. In *IEEE/CVF Conference on*
752 *Computer Vision and Pattern Recognition (CVPR): CVPR*. Institute of Electrical and Electronics
753 Engineers (IEEE), 2024.
- 754
- 755 Jianlin Su, Murtadha Ahmed, Yu Lu, Shengfeng Pan, Wen Bo, and Yunfeng Liu. Roformer: Enhanced
transformer with rotary position embedding. *Neurocomputing*, 568:127063, 2024.
- 756
- 757 Yu Sun, Xiaolong Wang, Zhuang Liu, John Miller, Alexei Efros, and Moritz Hardt. Test-time training
with self-supervision for generalization under distribution shifts. In *International conference on*
machine learning, pp. 9229–9248. PMLR, 2020.

- 756 Yansong Tang, Dajun Ding, Yongming Rao, Yu Zheng, Danyang Zhang, Lili Zhao, Jiwen Lu, and Jie
757 Zhou. Coin: A large-scale dataset for comprehensive instructional video analysis. In *Proceedings*
758 *of the IEEE/CVF Conference on Computer Vision and Pattern Recognition*, pp. 1207–1216, 2019.
759
- 760 Stefanie Tellex, Thomas Kollar, Steven Dickerson, Matthew R. Walter, Ashis Gopal Banerjee, Seth
761 Teller, and Nicholas Roy. Understanding natural language commands for robotic navigation
762 and mobile manipulation. In *Proceedings of the Twenty-Fifth AAAI Conference on Artificial*
763 *Intelligence*, AAAI’11, pp. 1507–1514. AAAI Press, 2011.
- 764 Zhan Tong, Yibing Song, Jue Wang, and Limin Wang. Videomae: Masked autoencoders are data-
765 efficient learners for self-supervised video pre-training. *Advances in neural information processing*
766 *systems*, 35:10078–10093, 2022.
- 767 An-Lan Wang, Kun-Yu Lin, Jia-Run Du, Jingke Meng, and Wei-Shi Zheng. Event-guided procedure
768 planning from instructional videos with text supervision. In *Proceedings of the IEEE/CVF*
769 *International Conference on Computer Vision*, pp. 13565–13575, 2023a.
- 770 Hanlin Wang, Yilu Wu, Sheng Guo, and Limin Wang. Pdpp: Projected diffusion for procedure
771 planning in instructional videos. In *Proceedings of the IEEE/CVF Conference on Computer Vision*
772 *and Pattern Recognition*, pp. 14836–14845, 2023b.
- 773 Limin Wang, Bingkun Huang, Zhiyu Zhao, Zhan Tong, Yinan He, Yi Wang, Yali Wang, and Yu Qiao.
774 Videomae v2: Scaling video masked autoencoders with dual masking. In *Proceedings of the*
775 *IEEE/CVF Conference on Computer Vision and Pattern Recognition*, pp. 14549–14560, 2023c.
776
- 777 Saining Xie, Chen Sun, Jonathan Huang, Zhuowen Tu, and Kevin Murphy. Rethinking spatiotemporal
778 feature learning: Speed-accuracy trade-offs in video classification. In *Proceedings of the European*
779 *conference on computer vision (ECCV)*, pp. 305–321, 2018.
780
- 781 Hu Xu, Gargi Ghosh, Po-Yao Huang, Dmytro Okhonko, Armen Aghajanyan, Florian Metze, Luke
782 Zettlemoyer, and Christoph Feichtenhofer. VideoCLIP: Contrastive pre-training for
783 zero-shot video-text understanding. In *Proceedings of the 2021 Conference on Empirical Methods*
784 *in Natural Language Processing (EMNLP)*, Online, November 2021. Association for Computa-
785 tional Linguistics.
- 786 Hu Xu, Saining Xie, Xiaoqing Tan, Po-Yao Huang, Russell Howes, Vasu Sharma, Shang-Wen Li,
787 Gargi Ghosh, Luke Zettlemoyer, and Christoph Feichtenhofer. Demystifying clip data. In *The*
788 *Twelfth International Conference on Learning Representations*, 2024.
789
- 790 Zhuoyi Yang, Jiayan Teng, Wendi Zheng, Ming Ding, Shiyu Huang, Jiazheng Xu, Yuanming Yang,
791 Wenyi Hong, Xiaohan Zhang, Guanyu Feng, et al. Cogvideox: Text-to-video diffusion models
792 with an expert transformer. *arXiv preprint arXiv:2408.06072*, 2024.
- 793 Xiaohua Zhai, Basil Mustafa, Alexander Kolesnikov, and Lucas Beyer. Sigmoid loss for language
794 image pre-training. In *Proceedings of the IEEE/CVF International Conference on Computer Vision*,
795 pp. 11975–11986, 2023.
796
- 797 He Zhao, Isma Hadji, Nikita Dvornik, Konstantinos G Derpanis, Richard P Wildes, and Allan D
798 Jepson. P3iv: Probabilistic procedure planning from instructional videos with weak supervision.
799 In *Proceedings of the IEEE/CVF Conference on Computer Vision and Pattern Recognition*, pp.
800 2938–2948, 2022.
- 801 Qi Zhao, Shijie Wang, Ce Zhang, Changcheng Fu, Minh Quan Do, Nakul Agarwal, Kwonjoon Lee,
802 and Chen Sun. Antgpt: Can large language models help long-term action anticipation from videos?
803 In *The Twelfth International Conference on Learning Representations*, 2024.
- 804 Yiwu Zhong, Licheng Yu, Yang Bai, Shangwen Li, Xueting Yan, and Yin Li. Learning procedure-
805 aware video representation from instructional videos and their narrations. In *Proceedings of the*
806 *IEEE/CVF Conference on Computer Vision and Pattern Recognition*, pp. 14825–14835, 2023.
807
- 808 Dimitri Zhukov, Jean-Baptiste Alayrac, Ramazan Gokberk Cinbis, David Fouhey, Ivan Laptev, and
809 Josef Sivic. Cross-task weakly supervised learning from instructional videos. In *Proceedings of*
the IEEE/CVF Conference on Computer Vision and Pattern Recognition, pp. 3537–3545, 2019.

A APPENDIX

In this appendix, we first present additional results on the step classification task (Appendix A.1.1) and procedure planning task (Appendix A.1.2). Then we discuss ablations of our model design, including the choice of attention mechanism (Appendix A.2.1), the choice of denoising steps (Appendix A.2.2), and the downstream task performance as we scale up the VEDiT model size (Appendix A.2.3). Furthermore, we provide the PyTorch (Ansel et al., 2024) implementation of VEDiT in Algorithm 1.

A.1 ADDITIONAL RESULTS

A.1.1 STEP CLASSIFICATION TASK

In this section, we present additional results on the COIN step classification task, which aims to predict the class labels of single-clip videos. In other words, this task tests only the capability of visual encoders, as the prediction model is not involved. Specifically, for step forecasting and task classification described in the main paper, we design the attentive pooler as a lightweight single cross-attention block with one query token to pool the video clip embedding (e.g., the predicted frame-level [CLS] tokens in SigLIP (Zhai et al., 2023)) into a single vector. For the COIN step classification task, we increase the depth of the attentive pooler by adding three additional self-attention blocks before the cross-attention block to aggregate information from the visual features, which we find further improves classification accuracy.

We compare our method, which uses off-the-shelf frozen visual encoders with a trainable attentive classifier, against baseline methods reported in previous works (Lin et al., 2022; Zhong et al., 2023). As shown in Table 7, our method with all five frozen encoders outperforms previous baselines. V-JEPA performs best among the two SSL-based video encoders (i.e., V-JEPA and VideoMAE). Increasing the resolution from 224 to 384 on V-JEPA further boosts accuracy. Additionally, due to the rich information encoded in patch-level tokens, V-JEPA achieves the best performance on the step classification task among all encoders. Moreover, SigLIP, pretrained on both image and text data, outperforms all other encoders except for V-JEPA, demonstrating the effectiveness of using visual-text aligned encoders for procedural activity understanding in instructional videos. However, as the prediction model is not involved, we do not put primary focus on this task in our paper.

Model	Pretraining Supervision	Pretrain Data	Top-1 Acc. (%)
Baselines			
SlowFast (Feichtenhofer et al., 2019)	Supervised: action labels	Kinetics (Kay et al., 2017)	32.9
TimeSformer (Bertasius et al., 2021)	Supervised: action labels	Kinetics (Kay et al., 2017)	48.3
ClipBERT (Lei et al., 2021)	Supervised: captions	COCO+VG (Chen et al., 2015; Krishna et al., 2017)	30.8
VideoCLIP (Xu et al., 2021)	Unsupervised: ASR	HT100M (Miech et al., 2019)	39.4
TimeSformer (Bertasius et al., 2021)	Unsupervised: ASR w. MIL-NCE	HT100M (Miech et al., 2019)	46.5
CLIP (Radford et al., 2021)	Unsupervised: captions	CLIP400M (Radford et al., 2021)	45.9
DistantSup (Lin et al., 2022)	Unsupervised: ASR + wikiHow	HT100M (Miech et al., 2019)	54.1
ProceduralVRL (Zhong et al., 2023)	Unsupervised: ASR	HT100M (Miech et al., 2019)	56.9
Ours (Frozen encoder w/ lightweight trainable attentive classifier)			
DINOv2 (Oquab et al., 2024)	Self-supervised	LVD-142M (Oquab et al., 2024)	57.9
V-JEPA@224 (Bardet et al., 2024)	Self-supervised	VideoMix2M (Bardet et al., 2024)	61.4
V-JEPA@384 (Bardet et al., 2024)	Self-supervised	VideoMix2M (Bardet et al., 2024)	62.7
VideoMAE (Tong et al., 2022)	Self-supervised	Kinetics400 (Kay et al., 2017)	58.5
SigLIP (Zhai et al., 2023)	Image+Text Pairs	WebLI (Chen et al., 2023)	<u>61.8</u>

Table 7: **Step classification on COIN dataset.** We **bold** and underline the best and the second best models in each task respectively. Our strategy of using strong frozen visual encoder with trainable attentive classifier outperforms all baseline methods.

A.1.2 PROCEDURE PLANNING TASK

In addition to the main results presented in Table 2, we show in Fig. 3 the comparison of our VEDiT and the vanilla transformer model in (Niu et al., 2024) as we increase the number of transformer blocks. We report success rate (SR), mean accuracy (mAcc), and mean IoU (mIoU) as evaluation metrics on the NIV, COIN, and CrossTask datasets. For a fair comparison, we keep all hyper-parameters the same, with the only change being the number of blocks. We observe that our VEDiT exhibits significantly better stability compared to the vanilla transformer blocks as we scale up the model size, without overfitting to the training set. This finding is consistent with our results in Fig. 7.

A.2 VEDiT MODEL ABLATIONS

A.2.1 CHOICE OF ATTENTION MECHANISM

In Fig. 4, we illustrate the differences between our default joint attention in each VEDiT block and self-attention and cross-attention. We denote the observed and unseen video clip embeddings as v^s or v^t . In self-attention, we concatenate v^s or v^t along the sequence dimension as a single input to the attention module. In contrast, cross-attention does not utilize self-attention within v^s or v^t . Here we conduct ablation study of these attention mechanisms with a prediction model of 3 VEDiT blocks. As shown in Fig. 5, our joint attention outperforms self-attention in step forecasting (50.3 vs. 49.7) and task classification (94.4 vs. 94.3) on the COIN dataset. This proves the usefulness of processing v^s and v^t differently through adaptive normalization layers before inputting to the attention module. In addition, due to the absence of self-attention within v^s or v^t , cross-attention performs the worst.

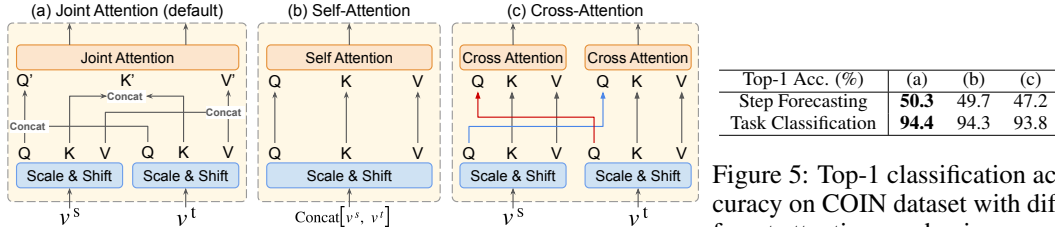


Figure 4: **Ablation of attention mechanisms**, including our default joint attention, self-attention, and cross-attention. We denote seen and target video clip embeddings as v^s and v^t respectively.

Figure 5: Top-1 classification accuracy on COIN dataset with different attention mechanisms.

A.2.2 CHOICE OF DENOISING STEPS

Previous work on masked token prediction, such as BERT (Kenton & Toutanova, 2019) for language and MAE (He et al., 2022) for images, can be considered single-step denoising, while diffusion models typically perform single-step denoising during training and multi-step denoising during inference. In this context, we conduct an ablation study on different denoising steps using diffusion timestamps sampled from the Flow Matching Euler Discrete Scheduler (Esser et al., 2024) in our VEDiT training on the COIN step forecasting task. The ablation study here is conducted with a prediction model of 3 VEDiT blocks, and we report the top-1 classification accuracy averaged over three independent runs in Fig. 6. Our results show that applying 20 to 40 denoising steps achieves better accuracy compared to single-step denoising (51.01 for 36 denoising steps v.s. 50.77 for single denoising step). This multi-step denoising allows us to reuse the same VEDiT architecture, with observed and target embeddings scaled and shifted by adaptive normalization layers at different timestamps, without drastically increasing the model’s trainable parameters. Additionally, we observe that timestamps that are too sparse (e.g., denoising steps of 4) or too dense (e.g., denoising steps greater than 44) make the model difficult to optimize. We default to use 24 denoising steps in our main paper as it achieves a good balance between computational cost and accuracy.

A.2.3 SCALABILITY OF VEDiT

Table 8 presents the model architecture details for 10 different scale models we implemented in our scalability results shown in Fig. 7. Specifically, we examined two different sets of hidden dimensions (i.e., 1280 and 2048), with varying numbers of VEDiT blocks ranging from 1 to 18. These parameter settings effectively cover model parameters from 62M to 1.77B (up to $\times 28$ larger in scale). We evaluated these models on the COIN step forecasting task, and the results are averaged over 5 runs. As shown in Fig. 7, with the same number of training epochs, a larger VEDiT model achieves a lower top-1 validation error compared to smaller VEDiT models. This demonstrates that VEDiT is scalable as we increase the model size.

918
919
920
921
922
923
924
925
926
927
928
929
930
931
932
933
934
935
936
937
938
939
940
941
942
943
944
945
946
947
948
949
950
951
952
953
954
955
956
957
958
959
960
961
962
963
964
965
966
967
968
969
970
971

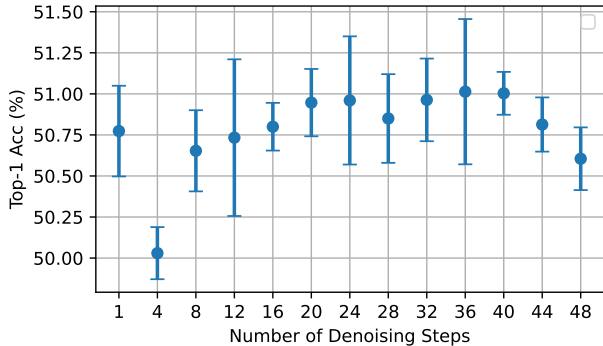


Figure 6: **Ablation of denoising steps.** We report the top-1 accuracy on COIN step forecasting task. A Denoising steps of 24 achieves a good balance between computational cost and accuracy. The numbers are averaged over 3 independent runs.

Model	# Train Params	Layers	Hidden Dim.	# Attn. Heads	Head Dim.
Hidden Dim. = 1280					
VEDiT-Single	62M	1	1280	20	64
VEDiT-Tiny	165M	3	1280	20	64
VEDiT-Small	342M	6	1280	20	64
VEDiT-Large	696M	12	1280	20	64
VEDiT-XL	1.05B	18	1280	20	64
Hidden Dim. = 2048					
VEDiT-Single	132M	1	2048	32	64
VEDiT-Tiny	418M	3	2048	32	64
VEDiT-Small	871M	6	2048	32	64
VEDiT-Medium	1.34B	9	2048	32	64
VEDiT-Large	1.77B	12	2048	32	64

Table 8: **Details of VEDiT models.** We introduce models of different number of transformer blocks (*i.e.*, layers) with two hidden dimension settings.

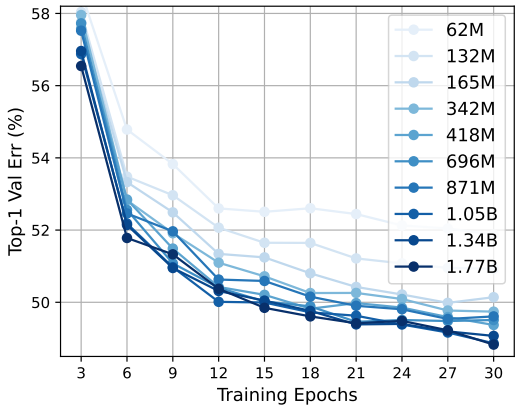


Figure 7: Ablation of different VEDiT model sizes. We report the top-1 validation error on COIN step forecasting task. Our VEDiT demonstrates good scalability as we scale up the model size *up to 28 times from 62M to 1.77B*. The numbers are averaged over 5 independent runs.

Algorithm 1 Simplified PyTorch Implementation for Each VEDiT Block

```

972
973
974
975 1 import torch
976 2 from torch import nn
977 3
978 4 class VEDiT(nn.Module):
979 5
980 6     def __init__(
981 7         self, dim, num_attention_heads, attention_head_dim, max_len):
982 8
983 9         # adaptive layernorm
984 10        self.norm1_seen = AdaLayerNormZero(dim)
985 11        self.norm1_target = AdaLayerNormZero(dim)
986 12
987 13        # normalization layers
988 14        self.norm2_seen = nn.LayerNorm(dim, elementwise_affine=False)
989 15        self.norm2_target = nn.LayerNorm(dim, elementwise_affine=False)
990 16
991 17        # FFN
992 18        self.ff_seen = FeedForward(dim=dim, dim_out=dim)
993 19        self.ff_target = FeedForward(dim=dim, dim_out=dim)
994 20
995 21        # joint attention
996 22        self.attn = JointAttention(
997 23            dim, num_attention_heads, attention_head_dim, max_len)
998 24
999 25    def forward(self, target_emb, seen_emb, temb, target_mask):
1000 26
1001 27        # 1. scale & shift
1002 28        norm_target, t_gate_msa, t_shift_mlp, t_scale_mlp, t_gate_mlp = \
1003 29            self.norm1_target(target_emb, emb=temb)
1004 30        norm_seen, s_gate_msa, s_shift_mlp, s_scale_mlp, s_gate_mlp = \
1005 31            self.norm1_seen(seen_emb, emb=temb)
1006 32
1007 33        # 2. joint attention
1008 34        seen_attn_output, target_attn_output = self.attn(
1009 35            hidden_states=norm_target,
1010 36            encoder_hidden_states=norm_seen,
1011 37            target_mask=target_mask)
1012 38
1013 39        # 3.1. target: gate, scale & shift
1014 40        target_emb = target_emb + t_gate_msa * target_attn_output
1015 41        norm_target_emb = self.norm2_target(target_emb)
1016 42        norm_target_emb = norm_target_emb * (1 + t_scale_nlp) + t_shift_nlp
1017 43
1018 44        # 3.2. target: feed forward
1019 45        ff_target_output = self.ff_target(norm_target_emb)
1020 46        target_emb = target_emb + t_gate_nlp * ff_target_output
1021 47
1022 48        # 4.1. seen: gate, scale & shift
1023 49        seen_emb = seen_emb + s_gate_msa * seen_attn_output
1024 50        norm_seen_emb = self.norm2_seen(seen_emb)
1025 51        norm_seen_emb = norm_seen_emb * (1 + s_scale_nlp) + s_shift_nlp
1026 52
1027 53        # 4.2. seen: feed forward
1028 54        ff_seen_output = self.ff_seen(norm_seen_emb)
1029 55        seen_emb = seen_emb + s_gate_nlp * ff_seen_output
1030 56
1031 57        return seen_emb, target_emb

```

```

1026
1027 Simplified PyTorch Implementation for JointAttention
1028
1029 1 import torch
1030 2 from torch import nn
1031 3 import torch.nn.functional as F
1032 4
1033 5 class JointAttention(nn.Module):
1034 6
1035 7     def __init__(
1036 8         self, dim, num_attn_heads, attn_head_dim, max_len):
1037 9
1038 10         self.heads, self.head_dim = num_attn_heads, attn_head_dim
1039 11         self.inner_dim = num_attn_heads * attn_head_dim
1040 12         self.max_len = max_len # max number of clips in procedural video
1041 13
1042 14         self.to_q = nn.Linear(dim, self.inner_dim, bias=True)
1043 15         self.to_k = nn.Linear(dim, self.inner_dim, bias=True)
1044 16         self.to_v = nn.Linear(dim, self.inner_dim, bias=True)
1045 17
1046 18         self.add_q = nn.Linear(dim, self.inner_dim, bias=True)
1047 19         self.add_k = nn.Linear(dim, self.inner_dim, bias=True)
1048 20         self.add_v = nn.Linear(dim, self.inner_dim, bias=True)
1049 21
1050 22         self.to_out = nn.Linear(self.inner_dim, dim, bias=True)
1051 23         self.add_out = nn.Linear(self.inner_dim, dim, bias=True)
1052 24
1053 25         self.rotary_emb = RotaryEmbedding(dim=dim) # rope
1054 26
1055 27     def forward(self, hidden_states, encoder_hidden_states, target_mask):
1056 28
1057 29         residual = hidden_states
1058 30         bs = hidden_states.shape[0]
1059 31
1060 32         # 1. concat q, k, and v from projected embeddings
1061 33         query = torch.cat([self.to_q(hidden_states),
1062 34                             self.add_q(encoder_hidden_states)], dim=1)
1063 35         key = torch.cat([self.to_k(hidden_states),
1064 36                             self.add_k(encoder_hidden_states)], dim=1)
1065 37         value = torch.cat([self.to_v(hidden_states),
1066 38                             self.add_v(encoder_hidden_states)], dim=1)
1067 39
1068 40         # 2. get positional indices of seen and target embeddings
1069 41         indices = torch.arange(0, self.max_len).repeat([bs, 1])
1070 42         seen_pos = indices[~target_mask].reshape([bs, -1])
1071 43         target_pos = indices[target_mask].reshape([bs, -1])
1072 44         input_pos = torch.concat([target_pos, seen_pos], axis=1)
1073 45
1074 46         # 3. apply rope to query and key
1075 47         query = self.rotary_emb.rotate(query, input_pos)
1076 48         key = self.rotary_emb.rotate(key, input_pos)
1077 49
1078 50         # 4. apply attention
1079 51         hidden_states = F.scaled_dot_product_attention(query, key, value)
1080 52         hidden_states = hidden_states.reshape(bs, -1, self.inner_dim)
1081 53         hidden_states, encoder_hidden_states = (
1082 54             hidden_states[:, : residual.shape[1]],
1083 55             hidden_states[:, residual.shape[1] :])
1084 56
1085 57         # 5. linear projection
1086 58         hidden_states = self.to_out(hidden_states)
1087 59         encoder_hidden_states = self.add_out(encoder_hidden_states)
1088 60
1089 61         return hidden_states, encoder_hidden_states

```
